

Observation and modeling of dynamic instabilities in the mutually pumped bird-wing phase conjugator in BaTiO₃

Ghazanfar Hussain and Stephen W. James

Department of Physics, University of Southampton, Southampton, SO9 5NH, UK

Robert W. Eason

Optoelectronics Research Centre, Department of Physics, University of Southampton, Southampton SO9 5NH, UK

Received May 28, 1990; accepted July 24, 1990

We observed dynamic instabilities in the phase-conjugate outputs from the mutually pumped bird-wing phase conjugator in BaTiO₃. We present experimental results that illustrate typical output characteristics and compare these with the results of a computer model that self-consistently determines all the relevant beam intensities within the crystal. The role of mutual erasure and the assisted routes to total-internal-reflection self-pumping are included within the model and are discussed in the context of the experimental results.

INTRODUCTION

In recent years a novel class of phase conjugator, the mutually pumped phase conjugator, has been demonstrated, in which two mutually incoherent beams interact within a photorefractive crystal, producing two simultaneous phase-conjugate outputs. The various types of mutually pumped phase conjugator may be distinguished by the number of total internal reflections that occur within the crystal: two in the mutually incoherent beam coupler,¹ one in the bird-wing phase conjugator² (BWPC), and none in the double-phase-conjugate mirror³; several other variants, including the bridge and frogs' legs, have also recently been reported.^{4,5}

Dynamic instabilities have previously been observed in several self-pumped phase-conjugate mirror (SPPCM) configurations.^{6,7} These instabilities result in fluctuations in phase-conjugate output power, which have been shown to depend on parameters such as input-beam geometry, beam intensity, and temperature. The cause of these instabilities is currently uncertain, because there are several possible explanations that can account for the oscillations in this complicated setup in which pump and signal beams are derived from a single input beam. Depending on the precise conditions, the observed outputs fluctuate either periodically or chaotically or in some complicated fashion with periods of regular oscillations giving way to chaotic behavior.

In this paper the observation of dynamic instabilities in the output of the BWPC is reported; these instabilities result from competition between the BWPC and SPPCM processes. This competition was noted by Ewbank² and could have been expected to occur, since the two processes have comparable thresholds.⁸ In addition to the experimental evidence, a phenomenological model was developed, based on observations of beam configurations within the crystal during a typical oscillation cycle.

In a configuration in which neither of the beams readily underwent self-pumping when separately incident, the for-

mation of the characteristic BWPC geometry enabled a self-pumping channel to develop from one of the beams, which is believed to have been brought above threshold by two-beam coupling (TBC) between fanned light and the light circulating within the BWPC channel.

Our proposed oscillation cycle is outlined in Fig. 1, while Fig. 2 shows the beam nomenclature used in the following discussion and in the model. Three principal interaction regions are considered: regions A and B, which determine the behavior of the BWPC process, and region C, where a TBC interaction between fanned light and the BWPC channel brings the SPPCM above threshold.

The grating written at region C diffracts light to region A, reducing the modulation ratio, m_A , and hence partially erasing the grating; thus the power that is traveling to region B in the BWPC channel is decreased, which results in an increased modulation ratio m_B and hence in more light traveling to region A. This increase in turn decreases the diffraction efficiency at region A still further. This feedback process leads to the BWPC process being brought below threshold, resulting in the subsequent decay of the induced SPPCM process. The cycle then repeats.

The computer simulation calculates the modulation ratio of the interacting beams at each region; i.e., for region A

$$m_A^2 = 4I_1 I_3 / I_A^2 \quad (1)$$

and for region B

$$m_B^2 = 4I_2 I_4 / I_B^2, \quad (2)$$

where I_A is the total intensity at region A and I_B the total intensity at region B. The diffraction efficiency at each region is

$$\eta_A = A m_A^2, \quad (3)$$

$$\eta_B = B m_B^2, \quad (4)$$

where

$$A = A_0 [1 - \exp(-t/\tau_A)], \quad (5)$$

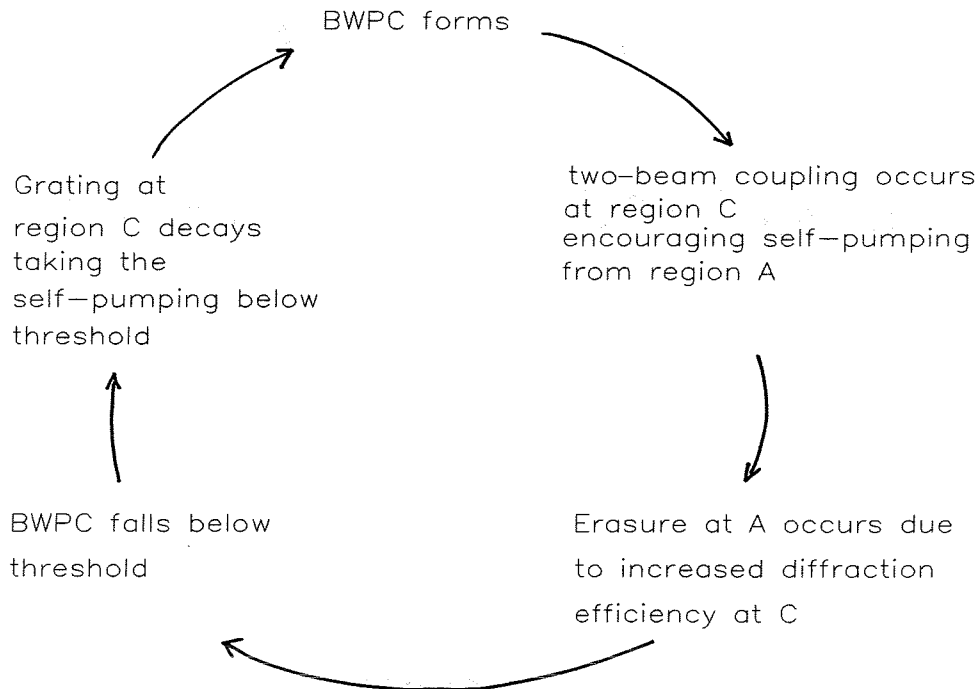


Fig. 1. Typical oscillation cycle.

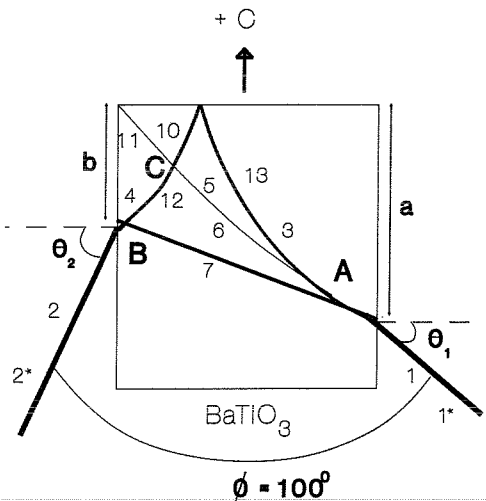


Fig. 2. Schematic of beam geometry with principal interaction regions and beam nomenclature.

$$B = B_0[1 - \exp(-t/\tau_B)], \quad (6)$$

where τ_A and τ_B are the response times of the gratings at regions A and B, respectively, and A_0 and B_0 are the relevant grating-strength factors, which include such parameters as the TBC gain constant and the angle between the interacting beams.⁹ On each time step the simulation calculates a self-consistent set of intensities and diffraction efficiencies and checks that a threshold condition, which can be compared with that of Ref. 7, for the diffraction efficiencies ($\eta_A, \eta_B \leq 0.001$) is satisfied. Once η_A reaches threshold, a grating at region C begins to grow with time constant τ_C , governed by an equation of the same form as Eqs. (5) and (6), and a self-pumping beam builds. When η_A falls below threshold the system is returned to its initial conditions, and the cycle is repeated.

A parameter that seemed experimentally important was the position of the undiffracted portion of beam 1, i.e., beam 7 relative to region B. This is thought to be a result of the extra erasure caused in region B by the presence of this beam. A parameter was introduced into the simulation that modified the contribution of I_7 to the total intensity (and hence the modulation ratio) at region B. It was found that in the absence of competition from the SPPCM this effect did not result in oscillations in the phase-conjugate output.

A typical output trace from the simulation is shown in Fig. 3. The parameter set used to obtain this trace was $I_1 = I_2$, $\tau_A = \tau_B = \tau_C = 10$ time steps, $A_0 = B_0 = C_0 = 0.8$. The results show qualitative agreement with experimental observations in that oscillations are observed and that there is a phase shift between the outputs (although not the experimentally observed 180°). However, variation of input-beam intensity ratios that are similar to those used experimentally does not reproduce the experimental results.

EXPERIMENTAL RESULTS

Figure 4 shows the experimental arrangement, which used an Ar⁺ laser operating in multilongitudinal mode at 514.5 nm and a single-domain crystal of BaTiO₃ of dimensions 6 mm × 6 mm × 6 mm. The laser output was spatially filtered and divided by beam splitter BS₁ into two beams of similar intensities. These beams, reflected and transmitted by BS₁, were incident upon opposite faces of the BaTiO₃ crystal to form a BWPC loop. The path length between the two beams I_1 and I_2 was arranged to be ≈ 1.5 m to ensure mutual incoherence. Beam splitters BS₂ and BS₃ were used to monitor the simultaneous phase-conjugate outputs, I_1^* and I_2^* . The input angles were $\theta_1 = 25^\circ$ and $\theta_2 = 55^\circ$ (measured outside the crystal). Both input

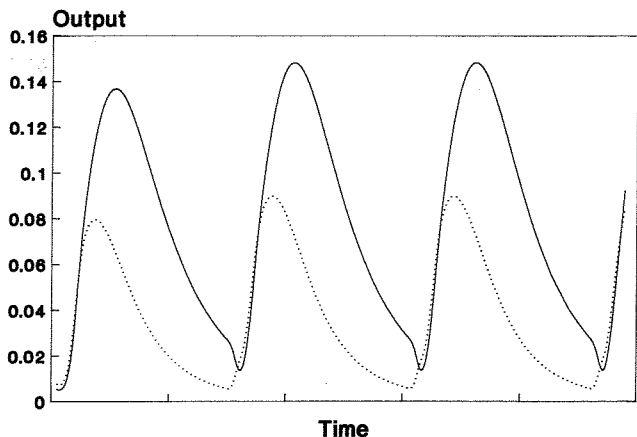


Fig. 3. Typical oscillation traces obtained by means of the computer model of the BWPC. Solid curve, I_1^* ; dotted curve, I_2^* .

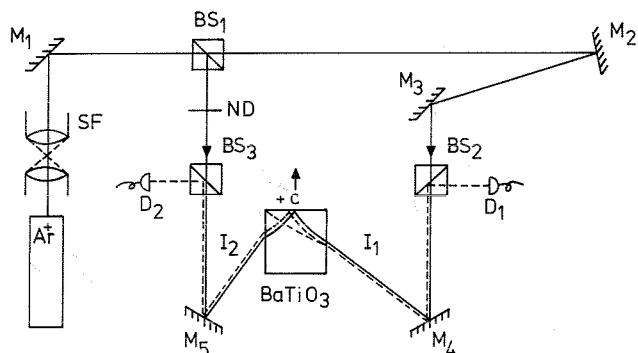


Fig. 4. Experimental arrangement used to observe dynamic instabilities in the mutually pumped BWPC. M_1 - M_5 , phase mirrors; SF, spatial filter; ND, variable neutral-density filter; D_1 , D_2 , photodiodes.

beams were e polarized to ensure maximum coupling strength.

Figure 5 shows a typical trace obtained when the parameters (as defined in Fig. 2) were set at $a = 3.8$ mm, $b = 3.5$ mm, $I_1 = 4.5$ mW, $I_2 = 1.5$ mW, i.e., a beam intensity ratio of $r = I_1/I_2 = 3$. It can be seen from the inset photograph that beam I_1 was directed at region B and hence strongly erased the fanning grating at that region. This prevented the BWPC loop formation. However, SPPCM configurations from beam I_1 did occur, although the output was highly unstable. This may be explained as follows: The SPPCM grating that formed resulted in reduced power in beam I_1 . This permitted beam I_2 to grow, promoting erasure of the SPPCM grating at region C, thus leading to a minimum in the monitored output. This in turn led to increased power in I_1 , and the cycle repeated. The maximum reflectivity in this case was low, $\approx 1\%$, and the fluctuations were not particularly regular (the average period was 13 ± 4 sec).

Figure 6 shows the traces obtained when parameter a was reduced to 3.6 mm, with b and r as before. It was observed here that the BWPC loop developed first in this case. Subsequently energy transfer between fanned light and light circulating within the BWPC loop occurred as a result of TBC in region C. When the SPPCM loop reached its highest level, beams I_3 and I_7 were at their lowest; consequently m_B was at its maximum. This resulted in more

light's being incident upon region A, reducing m_A , thus causing erasure at C and the subsequent decay of SPPCM. The cycle then repeated.

With this particular parameter set, the oscillation cycle resulted in stable periodic pulsations. The average period of the oscillation of I_1^* was 21 ± 0.7 sec. The maximum reflectivity measured from the highest peak was again low, $\approx 1\%$. Beam I_2^* had an average period of 21 ± 1 sec and a maximum reflectivity of only 0.2%. Figure 6 shows that the outputs I_1^* and I_2^* are almost 180° out of phase. This is the result of the nature of the sequential formation of BWPC and SPPCM processes.

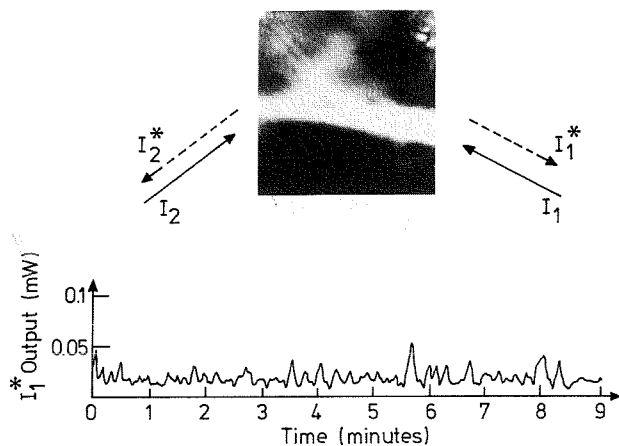


Fig. 5. Output obtained with parameters $a = 3.8$ mm, $b = 3.5$ mm, $I_1 = 4.5$ mW, $I_2 = 1.5$ mW.

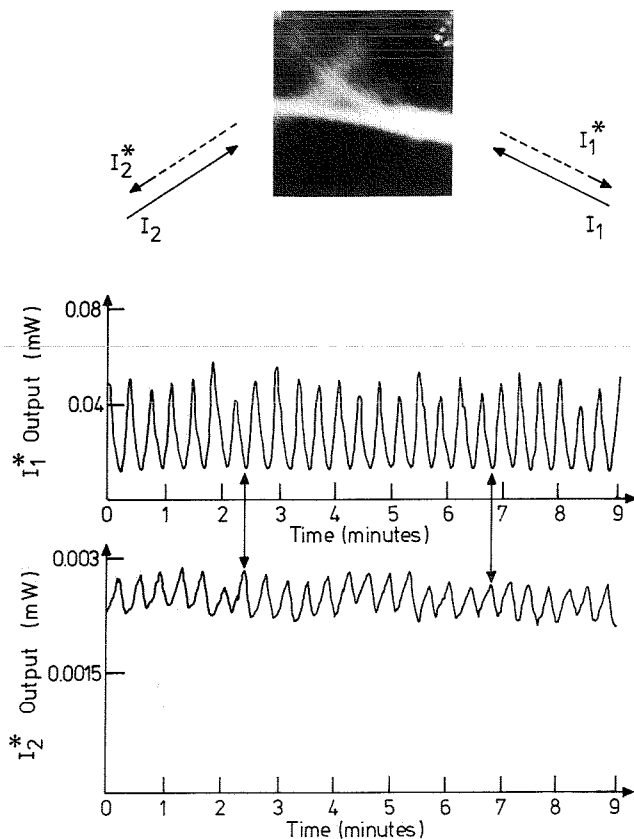


Fig. 6. Periodic oscillations obtained with $a = 3.6$ mm, $b = 3.5$ mm, $I_1 = 4.5$ mW, and $I_2 = 1.5$ mW.

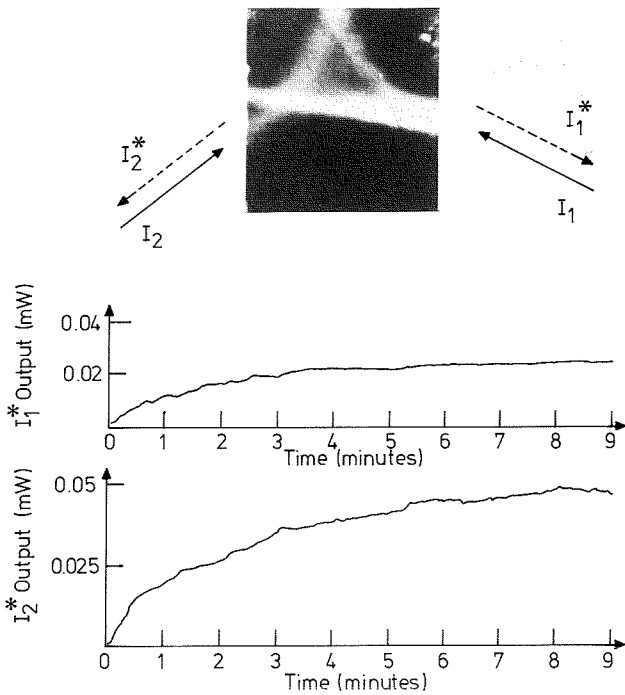


Fig. 7. Outputs obtained with $a = 3.2$ mm and other parameters as in Fig. 6.

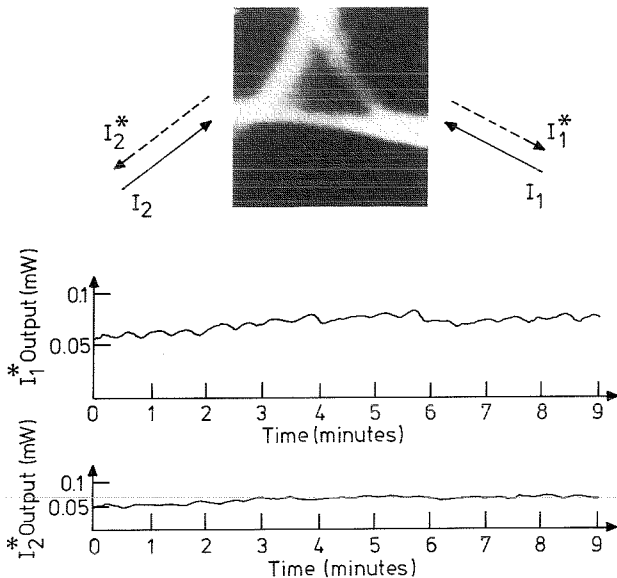


Fig. 8. Output traces behind with beam intensity ratio $r = I_1/I_2 = 1.5$ and other parameters as in Fig. 6. Note that large-scale oscillations are now absent.

Figure 7 shows the situation in which parameter a is reduced further to 3.2 mm (all other parameters remaining unchanged), causing region B to be shifted upward. In this arrangement we observed an overall increase in reflectivity from the BWPC loop. SPPCM configurations were not observed here, which may be because of the dominant presence of the BWPC loop, causing less fanned light to be available for SPPCM formation.

Finally, Fig. 8 shows the output traces with the same beam configuration as that used in Fig. 6 but with the beam intensities $I_1 = 5.0$ mW, $I_2 = 3.4$ mW, and $r = 1.5$. With this intensity ratio, beam I_2 formed stronger fanning

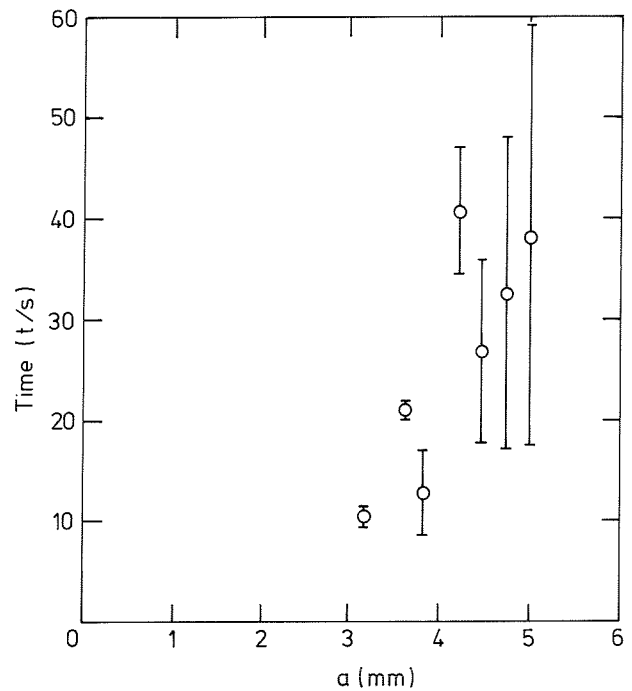


Fig. 9. Graph of parameter a versus period of oscillation. Note that regular oscillations occur only for limited values of a .

gratings, and therefore a strong BWPC was observed. However, self-pumping never became significant, and therefore we did not observe any competition between the two processes. It is observable in Fig. 8 that small perturbations may be present because of SPPCM competition, but these do not lead to oscillations as in Fig. 6.

In summary, Fig. 9 describes the analysis of the oscillation of I_2^* at different values of the parameter a , which is plotted on the horizontal axis. The vertical axis represents the period of the oscillation. It is seen that the standard deviation in the periodicity is large at larger values of the parameter a . At $a = 3.6$ mm, the amplitude and periodicity of both beams I_1^* and I_2^* were regular, as shown in Fig. 6.

CONCLUSION

We observed dynamic instabilities in the phase-conjugate outputs from a mutually pumped BWPC in BaTiO_3 . The outputs observed show both regular and irregular oscillations, depending on the precise experimental geometry chosen. However, the overall reflectivities observed were low and may have been due to the particular angular arrangement used to obtain oscillations and to the intensity ratio of the input beams. These results were compared with the results of a computer simulation, and, while not all the experimental features are predicted, the simple phenomenological model developed does predict oscillatory outputs in the presence of competition between the BWPC and SPPCM processes.

ACKNOWLEDGMENTS

We are grateful to the government of Pakistan and the overseas research scheme for a studentship for G. Hussain and to the Science and Engineering Research Council for

funding the research of S. W. James. We are also grateful to A. Walker of Heriot-Watt University for the loan of the BaTiO₃ crystal.

REFERENCES

1. R. W. Eason, and A. M. C. Smout, *Opt. Lett.* **12**, 15 (1987).
2. M. D. Ewbank, *Opt. Lett.* **13**, 47 (1988).
3. S. Sternklar, S. Weiss, M. Seger, and B. Fischer. *Opt. Lett.* **11**, 528 (1986).
4. A. A. Zozulya, A. V. Mamaev, and P. N. Lebedev, in *Digest of Topical Meeting on Photorefractive Materials, Effects, and Devices* (Optical Society of America, Washington, D. C., 1990), p. 307.
5. Qi-Chi He and J. G. Duthie, in *Digest of Topical Meeting on Photorefractive Materials, Effects, and Devices* (Optical Society of America, Washington, D.C., 1990), p. 342.
6. A. M. C. Smout, R. W. Eason, and M. C. Gower. *Opt. Commun.* **25**, 77 (1986).
7. P. Günter, E. Voit, and M. Z. Zha, *Opt. Commun.* **55**, 210 (1985).
8. Qi-Chi He, *IEEE J. Quantum Electron.* **24**, 2507 (1988).
9. A. M. C. Smout and R. W. Eason. *Opt. Lett.* **12**, 498 (1987).

